Science Forum (Journal of Pure and Applied Sciences)

Journal Homepage: https://atbu.edu.ng/science-forum/

Structural and Electronic Properties of Metal Halide Perovskite $CsSnBr_3$ for Optoelectronic Applications

Mohammed Buba, Ishaku Hamidu Midala, Jafaru Mohammed
Department of Science Laboratory Technology Federal Polytechnic Mubi Adamawa State

ABSTRACT

The structural and electronic properties of the Sn-based inorganic metal halide perovskite $CsSnBr_3$ are calculated and explored in depth using first-principles density functional theory (DFT). The Wu-Cohen (WC)-Generalized Gradient Approximation (GGA) based on the full-potential linearized augmented plane-wave (FPLAPW) method is used to optimize the geometry structure of the unit cell and then find the accurate optoelectronic properties of $CsSnBr_3$. Analysis of structural optimization results revealed that the lattice parameters (a^0 = 5.776 Å) and unit cell volume of $CsSnBr_3$ are exactly consistent with the experiments reports. Based on the results of band structures and density of states, $CsSnBr_3$ is found to be a nonmagnetic semiconductor with a suitable direct band gap of (E_g = 0.610 eV) along the R symmetry point. The results attained in the present study, include the stable crystal structure and the highly accurate electronic properties such as appropriate direct band gap which allow high absorption of visible radiation. This has confirmed the possible utilization of $CsSnBr_3$ materials in novel optoelectronics applications such as photovoltaic solar cells, photosensors, photodetectors, photodiodes, and other related optoelectronics devices.

ARTICLE INFO

Received 10 August 2023
Received in Revised Form 18 August 2023
Accepted 19 August 2023
Published 30 October 2023
Available online: 30 October 2023

KEYWORDS

Inorganic materials,
Metal halide perovskites,
Semiconductors,
Optoelectronics,
WC method

I. I NTRODUCTION

In the last few years, the distinctive family of halide perovskite solar cells (HPSCs) with an exclusive chemical formula (ABX_3) has attracted extreme interest as excellent spectra absorbers for photovoltaics and other novel optoelectronics applications. According to the sort of ion or element that occupies the A-site, the ABX_3 family can be classified into two famous classes of halide compounds:

(i) organic-inorganic halide perovskites and

(ii) (ii) all-inorganic halide perovskites.

The crystal of the first class contains organic ions [A = Methylammonium (MA), (CH_3NH_3) BX_3; formamidinium (FA), $(HC(NH_2)_2BX_3]$.

While, in all-inorganic halide perovskites, A-site is often occupied by a metallic element (A = Metal). The second class is considered one of the most studied compounds during the current era, where various inorganic HPSCs with ABX_3 (A = K, Rb, Cs; B = Metal; X= Halogen) have been created and investigated.

Besides studying their unique characteristics like flexible crystal structure, tunable semiconducting band-gap (Eg < 2.5 eV) [1], high charge-carrier mobility, large optical absorption coefficient, and high composition stability [2], research also seeks promising and multi-faceted thermal, and electrical and optical applications that give an extraordinary power-conversion efficiency (~24.0 %) in photovoltaic solar cells technologies [3].

Corresponding Author: Mohammed Buba ✉ mohdbuba@gmail.com ✉ Department of Science Laboratory Technology Federal Polytechnic Mubi Adamawa State

Photovoltaic solar cells are novel devices utilized mainly to convert free solar radiation into an electrical current through the photovoltaic effect. These devices present an optoelectronics design based on the combination of two semiconductor slabs with different electron concentrations [1]. As shown in (Fig. 1) these slabs build mainly from two different electrical materials that can be characterized as N-type semiconductor material owning an excess of negative charges, i.e. electrons, and P-type semiconductor material having an excess of positive charges, i.e. holes. As a result, when both N-type and P-type slabs are in contact, some energetic electrons flow from the N-type slab to the P-type slab, and some energetic holes flow conversely from the P-type slab to the N-type slab, which produces a diffusion current through the P-N junction. Moreover, the fixed ions near the two limits of the P-N junction generate an electric field in the opposite direction to the diffusion of these charges, which leads to the generation of drift current.

It is well known that the potential barriers established at the P-N junction as a result of the balance between this drift current and diffusion current at equilibrium, which makes the net current that flows through this structure equal to zero [4]. When the incident solar radiation strikes the surface of solar cells, the N-type electrons absorb the energy carried by its photons, which breaks their chemical bonds and creates electron-hole pairs in the N-type material.

These two charge carriers are pushed up by the electric field, causing them to flow through the P-N junction solar cell, and if a load is connected, an electric potential difference between the terminals of the solar cell will be established, which generates an electric current flowing through the external electrical load in the outer circuit.

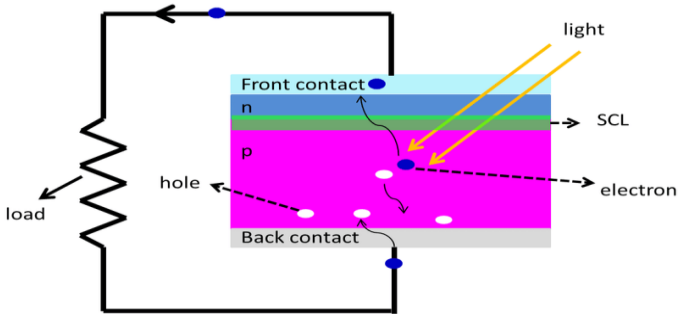

Fig.1. The photovoltaic effect and schematic illustration of P-N junction solar cell.

Therefore, the current challenge is to synthesize ABX_3 solid materials to provide suitable properties, including notable chemical stability at high temperatures, high electrical power conversion efficiency, broad emission, and tunable semiconducting E_g [5].

Motivated by the effect of A- and B-site substitution in ABX_3 unit cells, we extended this concept to produce a promising compound of $CsSnBr_3$ and explore its structural, and optoelectronic properties. Recently, several research studies have been done on numerous cubic compounds within the ABX_3 family, which is the most common structure in materials science and solid-state physics. Due to the possibility of substituting the three positions A, B, and X in ABX_3 with suitable metallic elements and halogens, respectively, these compounds can have all the potential to become promising materials with multifunctional properties [6].

Thus, most ABX_3 compounds can have remarkable performances in many fields of future applications, such as in photovoltaic solar cells. memories, sensors, and diode devices [4] electrodes, as well as ferroelectricity, superconductivity, and piezoelectricity applications [6]. These physical properties have attracted the widespread attention of scientists, engineers, and researchers to devote enormous efforts to these ABX_3 materials to investigate and

detect novel and useful properties for different future
applications [7].

In this work, to contribute and develop the materials research in this field as well as to explore new properties among the HPSC compounds that are not yet predicted experimentally or theoretically, we have intended to investigate the main physical properties of ABX_3 by choosing its sites as A is an alkali-metal, i.e. Cesium atom (A = Cs), B is post-transition metal (B = Sn) and X is a halogen element (X = Br).

This study proves a distinguished contribution in this field by examining the effect of site substitution (A = Cs, B = Sn) and applying the WC method on the structural and optoelectronic properties of ABX_3 compared to the published properties of related halide perovskites. The main goal of this study is to provide GGA theoretical bases to realize all these physical properties of Cesium bromide $CsSnBr_3$ and their dependence on the type of B-site.

All these calculations were carried out by utilizing the WC method based on the Generalized Gradient Approximation (GGA), to well examine the structural, electronic, and optical properties of $CsSnBr_3$. As a result of this work and based on their obtained chemical and physical properties, we can expect the possible applications of $CsSnBr_3$ halide perovskites in photovoltaic solar cells, photodetectors, photodiodes, and other related optoelectronics.

Computational methods

The ground state properties of CsSnBr3 are calculated using the first-principles density functional theory (DFT) [8][18], as executed in the WIEN2k [9] package. Full-potential linearized augmented plane-wave (FP-LAPW) method is utilized. The Wu-Cohen (WC) [10] method based on the Generalized Gradient Approximation (GGA) [11][21] is implemented to modulate the structural and optoelectronic properties of this compound. Non-spin-polarized versions of the WCGGA calculations are performed to obtain the appropriate results of these properties.

In the PFLAPW method, the unit cell of $CsSnBr_3$ contains two main regions; the first of which is a spherical region, muffin-tin (MT), where the potential is expected to be spherically symmetric, this region is definite by ($r \leq RMT$) where RMT is the muffin-tin radius. In all WC-GGA calculations, the RMT values of the individual elements in $CsSnBr_3$ are set as [RMT (Cs) = 2.2, RMT (Sn) = 2.0 and RMT (Br) = 1.8 a.u.]. In the MT region, the solution of the Schrödinger equation is given by a radial function times a spherical harmonic, whereas in the interstitial region (IR), the potential is considered constant and the Schrödinger equation is solved by plane wave functions.

The ground state energy convergence to (0.00001 Ry) was achieved using the total number of (k-points = 2000) in the first Brillouin zone (BZ) with a cutoff value (RMTKmax = 8.0), where RMT corresponds to the smallest MT radius and Kmax is the largest reciprocal lattice vector [9]. The structural optimizations of CsSnBr3 were carried out as a first stage, where the unit cell energy has been varied concerning its unit cell volume.

Results and discussion

As an initial utilization of the skills provided by the WIEN2k code, the optimized structural parameters of perovskite $CsSnBr_3$ are obtained from the $Energy$ vs. $Volume$ calculation in nonmagnetic (NM) and ferromagnetic (FM) phases. Fig. 2 shows the predicted results of

structural optimization by fitting the variation of the total energy per unit cell of $CsNBr_3$ as a function of its corresponding volume using the Murnaghan equation of state:

$$E - E_0 = \frac{B_0 V}{B_0'}\left(\frac{(V_0/V)^{B_0'}}{B_0'-1} + 1\right) - \left(\frac{B_0 V_0}{B_0'-1}\right) \quad \text{..... (1)}$$

where, E = the total energy per unit cell of $CsNBr_3$, E_0 = the ground state energy, E = the unit cell volume of $CsNBr_3$, V_0 = the equilibrium unit cell volume with lattice constants of ($a_0 = b_0 = c_0$), B_0 = the bulk modulus, and B_0' = the pressure derivative of bulk modulus.

The crystal structure of $CsSnBr_3$ in the NM phase is more stable than in the FM phase because it shows less energy ($ENM < EFM$). Table 1 summarizes the structural data of $CsSnBr_3$ extracted from the optimization calculations compared with the available experimental and previous DFT results.

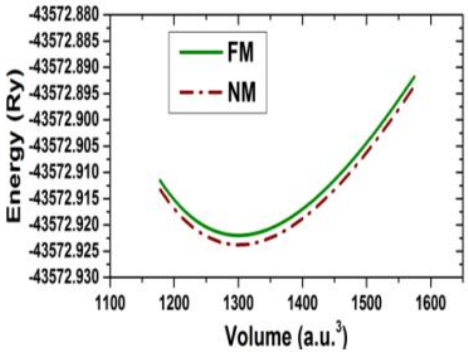

Fig. 2. The optimized energy vs. unit cell volume of metal halide perovskite $CsSnBr_3$.

Table 1. The optimized structural data of metal halide perovskite $CsSnBr_3$.

Parameter	Present	Other [25,26]
S. G.	Pm-3m	Pm-3m
a_0 (Å)	5.776	5.883, 5.800
V_0 (Å3)	192.7	
B_0 (GPa)	22.19	
B_0' (GPa)	4.634	
TF	1.006	
Sn–Br (Å)	2.888	
E_0 (Ry)	-43572.92	
E_g (eV)	0.610	0.600, 0.626

Because of these, it can be concluded that the obtained value of a_0 is in good agreement with those results. Also, the value of $B0$ illustrates the mechanical stiffness of $CsSnBr_3$ which makes it more rigid material and less compressible. Alike expectation was reported for analogous metal halide perovskites within GGA studies [12] Also, the atomic distances and positions in the cubic unit cell of $CsSnBr_3$ are shown in (Fig. 3), Cs at 1a (0,0,0), Sn at 1b (0.5,0.5,0.5) and Br at 3d (0.5,0,0), (0,0.5,0) and (0,0,0.5). Moreover, two important characteristics that determine the suitability of $CsSnBr_3$ material for the manufacture of photovoltaic solar cells and related optoelectronics devices have quantum efficiency and chemical stability. The tolerance factor [13] evaluates the chemical stability of $CsSnBr_3$ using ionic radii, as:

$$T_F = \frac{0.71(r_{Cs}+r_{Br})}{(r_{Sn}+r_{Sn})} \quad \text{..... (2)}$$

where, (r_{Cs} = 2.02 Å) in the XII-coordinate system, and (r_{Sn} = 0.89 Å) and (r_{Br} = 1.82 Å) in the VI coordinate system [14]. As a result of applying this formula, it is found that the stable cubic crystal structure of halide perovskite $CsSnBr_3$ gives a value close to the standard value (TF ≈ 1.00), which matches also the (Pm-3m; #221) symmetry

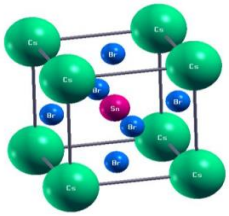

Fig. 3. The cubic crystal structure of metal halide perovskite CsSnBr3.

To study the electronic properties of $CsSnBr_3$, its 2D charge density, band structure, total density of states (TDOS) and partial density of states (PDOS) have been calculated
and discussed deeply as follows. First, Fig. 4 represents the charge density in the (100) plane of the unit cell of $CsSnBr_3$, which gives a clear picture of the chemical bonding nature between the three
atoms Cs, Sn, and Br in their unit cell $CsSnBr_3$ as well as allows to explain the charge transfer mechanisms through these bonds. It can be seen that there is a formation of orbital hybridizations between p-states of cations Sn-5p and anions Br-4p. The condensed contour lines around Sn and Br indicates their covalent bond nature whereas the formation of other bonds Cs– Br have an ionic nature with minor contour lines.

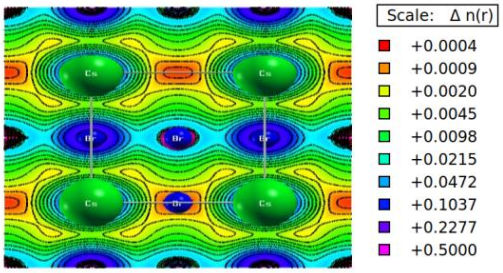

Fig. 4. The 2D charge density in (100) plane for the unit cells of metal halide perovskite $CsSnBr_3$.

Second, an important parameter of semiconductors is the value of band gap (Eg), which can be
extracted from the results of calculated band structures, which can be used to evaluate the potential
of this compound for optoelectronics applications. Fig. 5 shows the calculated band structures of
CsSnBr3 along their high cubic symmetry points within the first BZ. The key remark here, that perovskite $CsSnBr_3$ shows semiconductor property with a direct E_g at an R-point of about (Eg ≈ 0.610
eV) in good agreement with the experimental value (e.g. ≈ 0.600 eV) and smaller than the GGA result
(E_g ≈ 0.626 eV) [15] The indirect E_g of $CsSnBr_3$ is located between the valence band maxima and conduction band minima, which both lie along the R symmetry point. Where, the valence band maxima line touches the Fermi level (EF = 0.0 eV). Compared with its analogous Ge and Pb-based halide perovskites [12], the narrow Eg shown by the $CsSnBr_3$ crystal increases its significance for P-N junction (Fig. 1) in optoelectronics devices and photovoltaic solar cells applications.

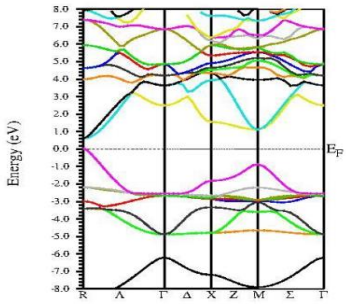

Fig. 5. The calculated band structures of metal halide perovskite $CsSnBr_3$.

Third, to evaluate the atomic contribution to the density of states and the nature of the atomic bonding in $CsSnBr_3$, the total density of states (TDOS), and partial density of states (PDOS)
are calculated using the WC method and shown in Figs. 6 and 7. It is obvious that TDOS (Fig. 6(a)) shows an E_g at the E_F, which also predicts the semiconducting behaviors obtained from the band
structures. Also, the different contributions come from the TDOS per atom of Cs, Sn, and Br to the TDOS per unit cell of $CsSnBr_3$ are plotted in (Fig. 6(b)).

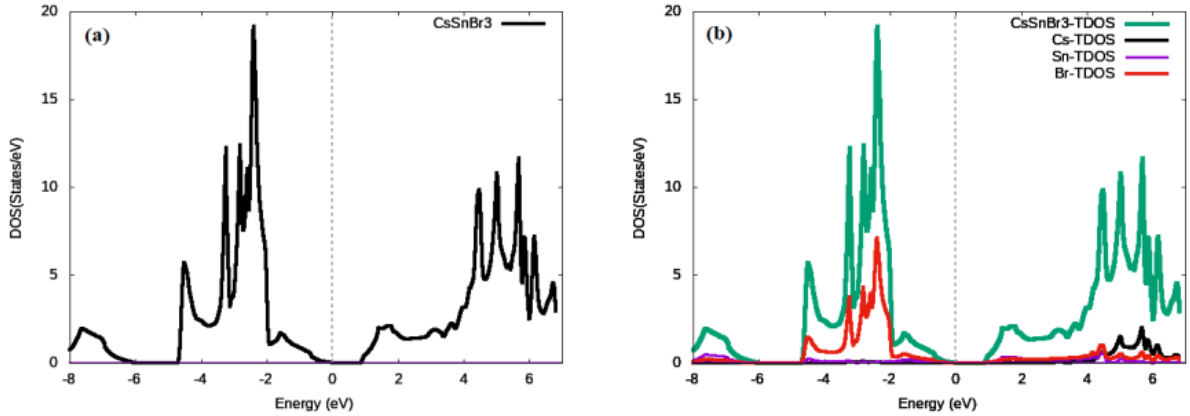

Fig. 6. The calculated total density of states; (a) TDOSs of CsSnBr3, and (b) TDOSs of Cs, Sn, and Br of atoms, per unit

Moreover, the PDOSs per atom (Fig. 7(a,b, c)) confirm that the valence bands create from the partial hybridizations between Sn (5s, 5p) and Br (4p) states extend between -5.0 eV and EF, whereas the conduction bands are generally dominated by the Sn (5p) and Br (4p) hybridizations. The top of valence bands is yielded by partial 5s and 4p states, Sn (5s) – Br (4p),
and the bottom of conduction bands are occupied by 5p and 4p states with no contribution come
from Cs (5p) and Cs (4d) states. The prediction of semiconducting property gives complete confidence of the tenability to develop such the proposed CsSnBr3 compound as promising candidate materials for novel light-emitting diodes, optoelectronic and photovoltaic technologies
[16]

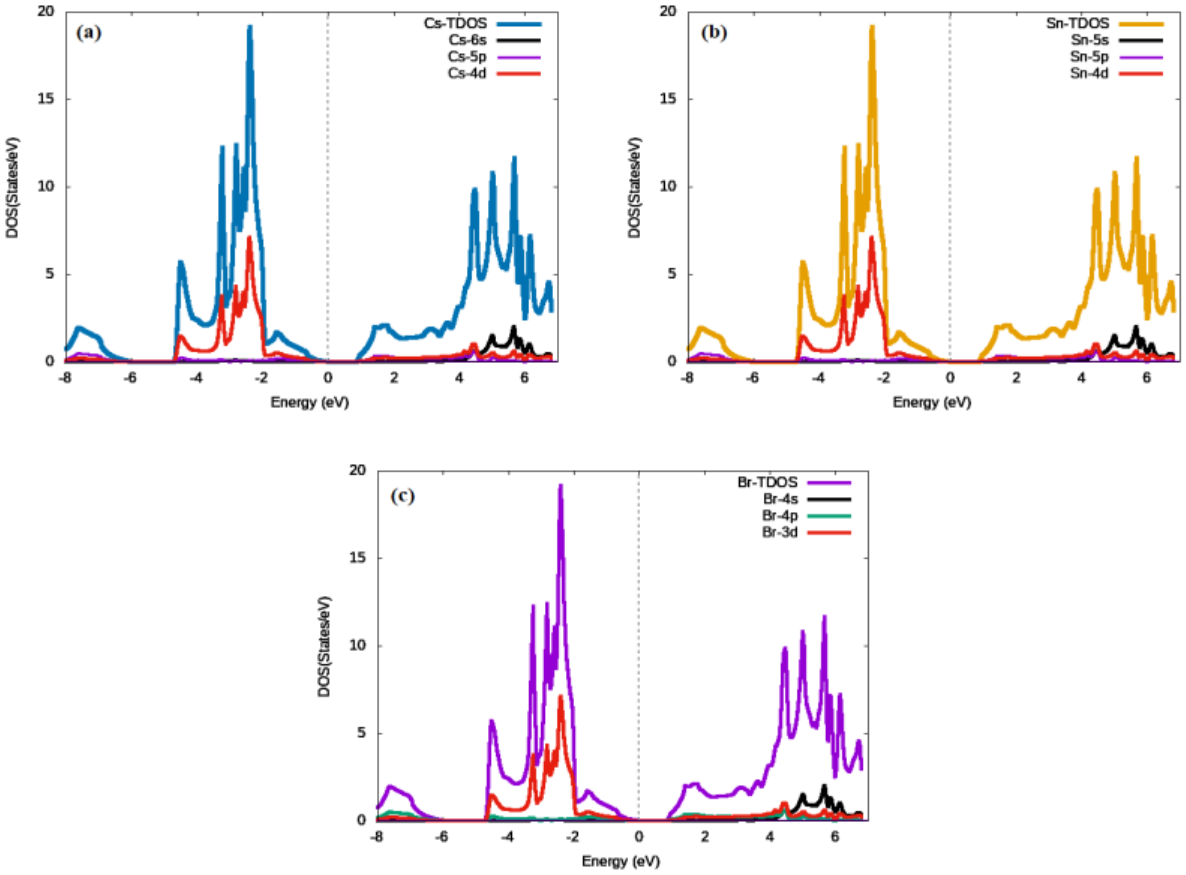

Fig. 7. The calculated partial density of states; PDOSs of (a) Cs, (b) Sn, and (c) Br, per atom in metal halide perovskite CsSnBr3.

Conclusions

In this work, the structural, electronic, and optical properties of all-inorganic metal halide perovskite $CsSnBr_3$ were examined for novel optoelectronics applications by execution of density
functional theory (DFT) based on the FP-LAPW-WIEN2k method. To highlight these properties, the WC method based on the Generalized Gradient Approximation (GGA) has been used in all
calculations. The results obtained from structural optimizations that were carried out using the WC method,

show that the compound $CsSnBr_3$ stable in cubic structure (Pm-3m; no. 221) with (a0 = 5.776 Å). Also, the calculation results of band structures, the density of states, and 2D charge density show that the present perovskite $CsSnBr_3$ exhibits nonmagnetic and semiconductor properties and characterized by an appropriate direct band gap of (Eg ≈ 0.610 eV) lie along the R-R symmetry point. Moreover, the results obtained for the optical properties, the real part of the dielectric function, the absorption coefficient $\alpha(\omega)$, the refractive index $n(\omega)$ and the reflectivity $R(\omega)$, confirm that the crystal of $CsSnBr_3$ is a good light absorber with high light absorption extends in the visible range.

Accordingly, the exclusive properties of $CsSnBr_3$, which include high structural stability, high ductility and elasticity, suitable value of

direct band gap, and high optical absorption make it a promising material for various novel applications. The present theoretical results provide a basis for the future experimental studies of Cs-based halide perovskites and related compounds, which have structural and optical properties that may be necessary in novel fields of optoelectronics industries such as photovoltaic solar cells, photodetectors, photodiodes, and other photovoltaic devices.

References

[1] J. A. Luceño-Sánchez, A. M. Díez-Pascual, and R. P. Capilla, "Materials for Photovoltaics: State of Art and Recent Developments," *Int. J. Mol. Sci. 2019, Vol. 20, Page 976*, vol. 20, no. 4, p. 976, Feb. 2019, doi: 10.3390/IJMS20040976.

[2] A. Kumar *et al.*, "Perovskites: transforming photovoltaics, a mini-review," *https://doi.org/10.1117/1.JPE.5.057402*, vol. 5, no. 1, p. 057402, Jan. 2015, doi: 10.1117/1.JPE.5.057402.

[3] G. Lozano, "The Role of Metal Halide Perovskites in Next-Generation Lighting Devices," *J. Phys. Chem. Lett.*, vol. 9, no. 14, pp. 3987–3997, Jul. 2018, doi: 10.1021/ACS.JPCLETT.8B01417/ASSET/IMAGES/LARGE/JZ-2018-01417D_0003.JPEG.

[4] S. Yun *et al.*, "New-generation integrated devices based on dye-sensitized and perovskite solar cells," *Energy Environ. Sci.*, vol. 11, no. 3, pp. 476–526, Mar. 2018, doi: 10.1039/C7EE03165C.

[5] D. Bharath Raja, K. Shanmuga Sundaram, and R. Vidya, "First principle study on hybrid organic-inorganic perovskite ASnBr3 (A = Formamidinium, Dimethylammonium and Azetidinium)," *Sol. Energy*, vol. 207, pp. 1348–1355, Sep. 2020, doi: 10.1016/J.SOLENER.2020.07.044.

[6] L. M. Herz, "Charge-Carrier Mobilities in Metal Halide Perovskites: Fundamental Mechanisms and Limits," *ACS Energy Lett.*, vol. 2, no. 7, pp. 1539–1548, Jul. 2017, doi: 10.1021/ACSENERGYLETT.7B00276/ASSET/IMAGES/LARGE/NZ-2017-00276E_0001.JPEG.

[7] W. Xiang and W. Tress, "Review on Recent Progress of All-Inorganic Metal Halide Perovskites and Solar Cells," *Adv. Mater.*, vol. 31, no. 44, p. 1902851, Nov. 2019, doi: 10.1002/ADMA.201902851.

[8] D. S. Sholl, "Density functional theory," *Electrocatal. Comput. Exp. Ind. Asp.*, pp. 117–138, 2010, doi: 10.1201/9781420045451.

[9] K. Schwarz, P. Blaha, and G. K. H. Madsen, "Electronic structure calculations of solids using the WIEN2k package for material sciences," *Comput. Phys. Commun.*, vol. 147, no. 1–2, pp. 71–76, Aug. 2002, doi: 10.1016/S0010-4655(02)00206-0.

[10] P. Hohenberg and W. Kohn, "Inhomogeneous electron gas," *Phys. Rev.*, vol. 136, no. 3B, p. B864, Nov. 1964, doi: 10.1103/PHYSREV.136.B864/FIGURE/1/THUMB.

[11] J. P. Perdew, K. Burke, and M. Ernzerhof, "Generalized Gradient Approximation Made Simple," *Phys. Rev. Lett.*, vol. 77, no. 18, p. 3865, Oct. 1996, doi: 10.1103/PhysRevLett.77.3865.

[12] M. Houari *et al.*, "Semiconductor behavior of halide perovskites AGeX3 (A = K, Rb and Cs; X = F, Cl and Br): first-principles calculations," *Indian J. Phys.*, vol. 94, no. 4, pp. 455–467, Apr. 2020, doi:

10.1007/S12648-019-01480-0/METRICS.

[13] V. M. Goldschmidt, “Die Gesetze der Krystallochemie,” *Naturwissenschaften*, vol. 14, no. 21, pp. 477–485, May 1926, doi: 10.1007/BF01507527/METRICS.

[14] R. D. Shannon and IUCr, “Revised effective ionic radii and systematic studies of interatomic distances in halides and chalcogenides,” *urn:issn:0567-7394*, vol. 32, no. 5, pp. 751–767, Sep. 1976, doi: 10.1107/S0567739476001551.

[15] M. A. Islam, M. Z. Rahaman, and S. K. Sen, “A comparative study of hydrostatic pressure treated environmentally friendly perovskites CsXBr3 (X = Ge/Sn) for optoelectronic applications,” *AIP Adv.*, vol. 11, no. 7, Jul. 2021, doi: 10.1063/5.0057287/990108.

[16] K. Ji *et al.*, “Halide Perovskite Light-Emitting Diode Technologies,” *Adv. Opt. Mater.*, vol. 9, no. 18, p. 2002128, Sep. 2021, doi: 10.1002/ADOM.202002128.